Highly Sensitive Chiral Analysis in Capillary Electrophoresis with Large-volume Sample Stacking with an Electroosmotic Flow Pump

Takayuki Kawai[*], Hiroshi Koino, Kenji Sueyoshi, Fumihiko Kitagawa[‡], and Koji Otsuka

Department of Material Chemistry, Graduate School of Engineering, Kyoto University, Katsura, Nishikyo-ku, Kyoto 615-8510, Japan

*To whom correspondence should be addressed.

Tel.: +81-75-383-2449, FAX: +81-75-383-2450

E-mail: t.kawai@kt2.ecs.kyoto-u.ac.jp

[‡]*Present address: Department of Frontier Material Chemistry, Graduate School of Science and Technology, Hirosaki University, Hirosaki, Aomori 036-8561, Japan*

Tel. and FAX: +81-172-39-3946

E-mail: kitagawa@cc.hirosaki-u.ac.jp

Abstract

To improve the sensitivity in chiral analysis by capillary electrophoresis without loss of optical resolution, application of large-volume sample stacking with an electroosmotic flow pump (LVSEP) was investigated. Effects of the addition of cyclodextrin (CD) into a running solution on the LVSEP preconcentration was theoretically studied, where the preconcentration efficiency and effective separation length would be slightly increased if the effective electrophoretic velocity ($v_{ep,eff,BGS}$) of the analytes was decreased by interacting with CD. In LVSEP-CD-modified capillary zone electrophoresis (CDCZE) and LVSEP-CD electrokinetic chromatography with reduced $v_{ep,eff,BGS}$, up to 1,000-fold sensitivity increases were achieved with almost no loss of resolution. In LVSEP-CD-modified micellar electrokinetic chromatography of amino acids with increased $v_{ep,eff,BGS}$, a 1,300-fold sensitivity increase was achieved without much loss of resolution, indicating the versatile applicability of LVSEP to many separation modes. An enantio-excess (EE) assay was also carried out in LVSEP-CDCZE, resulting in successful analyses of up to 99.6% EE. Finally, we analyzed ibuprofen in urine by desalting with a C18 solid-phase extraction column. As a typical result, 250 ppb ibuprofen was well concentrated and optically resolved with 84.0–86.6% recovery in LVSEP-CDCZE, indicating the applicability of LVSEP to real samples containing a large amount of unnecessary background salts.

Introduction

Chiral compounds are recognized to play important roles in chemistry, biology, medicine, and pharmacology [1–3], so that the analytical methods for the chiral compounds require the high sensitivity, high optical resolution, and short analysis time. Among several chiral separation methods, such as high-performance liquid chromatography (HPLC), gas chromatography, and capillary electrophoresis (CE), CE exhibits high resolution with little sample consumption in a short analysis time. Several separation modes have been developed for chiral separation in CE, including micellar electrokinetic chromatography (MEKC), cyclodextrin (CD)-modified capillary zone electrophoresis (CDCZE), CD electrokinetic chromatography (CDEKC), CD-modified MEKC (CDMEKC), affinity capillary electrophoresis (ACE), and nonaqueous CE (NACE) [4–6]. However, the concentration sensitivity is quite poor because of the short optical path length and the small injection volume of sample solution.

To overcome such the drawback of CE, several online sample preconcentration techniques have been developed [7–21]. Although up to 1,000-fold sensitivity increases have been achieved in chiral analysis [7–16], optimization of the preconcentration conditions is usually required because the resolution was reduced due to the decrease in the effective separation length accompanying the increase in the sample injection volume [17–19]. Since the enantioseparation is not so easy without the optimal electrolyte composition, additional optimization of the preconcentration condition is one of the most serious disadvantages. Moreover, highly efficient preconcentration techniques often require multi-step procedures [16,20], which are quite bothersome and often cause the reduction in the analytical reproducibility. Hence, we focused on an online sample preconcentration technique using field amplified sample stacking,

large-volume sample stacking with an electroosmotic flow (EOF) pump (LVSEP) [21–23], which provides the high sensitivity with almost no loss of resolution in a simple experimental procedure. In our previous work [22], up to 780-fold sensitivity increases were achieved with good separation performance in the CE analysis of oligosaccharides. Moreover, we did not need to optimize the sample injection volume, because the sample filled in the whole capillary could be concentrated. Thus, the application of LVSEP to the chiral analysis in CE is expected to improve the sensitivity with high enantioseparation efficiency and to minimize the optimization procedure of the experimental conditions and the multi-step preconcentration procedure.

In spite of the high preconcentration and separation ability of LVSEP, there has been no report on the separation performance in combining LVSEP with any separation modes except for the most basic separation mode, capillary zone electrophoresis (CZE). In LVSEP, the separation performance is determined by the inversion position of the sample migration where the EOF velocity and electrophoretic velocity of the analyte in a background solution (BGS) is balanced [23]. Hence, the change in the effective electrophoretic mobility in the different separation mode can cause the increase or decrease in the resolution. It is important to consider the effect of the separation mode on the resolution both theoretically and experimentally.

Our aims in this study are to clarify the effects of the separation mode on the resolution in LVSEP and to achieve the efficient improvement of the concentration sensitivity without loss of optical resolution and without complicated experimental procedures including the optimization steps. Theoretical investigation on the resolution in the LVSEP-applied chiral analysis using CDs as chiral selectors was performed by estimating the inversion position, which is expected to directly affect the effective

separation length. Three enantioseparation modes, CDCZE, CDEKC, and CDMEKC, were carried out to evaluate the performance of the sensitivity improvement and the enantioseparation. An enantio-excess (EE) assay was also carried out in LVSEP-CDCZE. Finally, we performed the analysis of a drug component dissolved in a urine matrix to show how to analyze real samples containing a large amount of unnecessary background salts. The purification using a C18 solid-phase extraction (SPE) column was applied for the LVSEP analysis of the urine sample.

Experimental Section

Materials and Chemicals.

A fused silica capillary was purchased from Polymicro Technologies (Phoenix, AZ, USA), poly(vinyl alcohol) (PVA, M_w = 88,000, 99% hydrolyzed) was obtained from Japan Vam and Poval (Osaka, Japan), warfarin was purchased from Dr. Ehrenstorfer GmbH (Augsburg, Germany), thiourea, (±)-abscisic acid, racemic ibuprofen, (S)-(+)-2-(4-isobutylphenyl)propionic acid ((S)-ibuprofen), 2,6-di-*O*-methyl-β-cyclodextrin (DM-β-CD), and 2,3,6-tri-*O*-methyl-β-cyclodextrin (TM-β-CD) were purchased from Wako (Osaka, Japan), quaternary β-cyclodextrin (QA-β-CD) and DL-leucine were purchased from Sigma-Aldrich (St. Louis, MO, USA), and all other reagents were purchased from Nacalai Tesque (Kyoto, Japan). All solutions were prepared with deionized water purified by using a Direct-Q System (Nihon Millipore, Japan), and filtered through a 0.45 μm pore membrane filter (Nacalai Tesque) prior to use.

Derivatization of Amino Acids

Amino acids were derivatized with fluorescein isothiocyanate (FITC) for laser-induced fluorescence (LIF) detection as in the previous report [24]. Briefly, 5 μL of 50 mM amino acids and 5 μL of 50 mM FITC dissolved in 50 mM borate buffer (pH 9.5) were mixed and left for 24 h at room temperature. The solution was diluted with deionized water or a BGS for the appropriate concentrations.

SPE Purification of Urine Sample

Urine samples spiked with ibuprofen were purified with a C18 SPE column (Inert Sep C18, GL science, Kyoto, Japan). Urine was sampled from a healthy male volunteer and filtered with a 0.45 μm pore membrane filter. Ibuprofen dissolved in methanol (1%, w/v) was spiked in the urine for certain concentration, followed by adjusting pH to around 3 by adding 6 M hydrochloric acid. After conditioning the SPE column with 1 mL methanol and 1 mL water, 500 μL of the urine sample was passed through the cartridge with a gentle gravity pressure at a flow rate of about 0.3 mL/min. The column was washed with 1.5 mL of water, 0.5 mL of 25 mM formic acid in ACN/water (20/80, v/v), and 1.5 mL of water again. Ibuprofen was then eluted with 0.5 mL of ACN. The eluent was lyophilized and the residue was diluted with 500 μL of water for the LVSEP analysis.

Capillary Coating

A fused silica capillary was coated with PVA in the same way as the previous papers [22,25,26]. Briefly, the capillary was activated and washed with 1 M NaOH and water, followed by the injection of a 5% PVA solution into the whole capillary. Both the

capillary ends were immersed in the same PVA solution and left at room temperature for 15 min. The PVA solution was then removed out of the capillary and the capillary was heated at 140 °C for 18 h under a nitrogen gas flow. The capillary was filled with deionized water and stored at room temperature. Prior to use, the capillary was flushed with a BGS for 15 min.

Apparatus

All CE experiments were performed on a P/ACE MDQ system (Beckman Coulter, Fullerton, CA, USA) equipped with a diode-array UV detector or a LIF detector. The LIF detector used in the LVSEP-CDMEKC analysis consisted of a 488 nm argon ion laser module and photomultiplier detector with a 520 nm band pass filter. UV detection was performed at 200 nm in LVSEP-CDCZE or 250 nm in LVSEP-CDEKC.

Analytical Procedure.

The capillary with total/effective lengths of 40/30 cm was employed in the CDCZE analysis and that of 60/50 cm in the CDEKC and CDMEKC analyses. They were conditioned with deionized water in applying LVSEP or with the BGS in the conventional CDCZE/CDEKC/CDMEKC analyses at 20 psi for 3 min prior to each run. Sample injections were performed with a pressure of 20 psi for 90 s (whole capillary injection) in the LVSEP-applied analyses or 0.3 psi for 3 s in the other conventional analyses. The applied voltage and the temperature were set at –30 kV and 25 °C, respectively, except in the CDCZE analysis of ibuprofen with voltage application of ‑25 kV.

Results and Discussion

Theoretical Consideration

In LVSEP-CDCZE/CDEKC/CDMEKC, the EOF-suppressed capillary is filled with a low ionic strength solution containing anionic analytes, whereas the inlet and outlet vials are filled with the high ionic strength BGS containing CD (Figure 1a). After applying the voltage, anionic analytes are concentrated at the sample matrix (SM)/BGS boundary by the difference in the electric field strength between the two zones. The focused analytes move toward the cathode and the BGS is introduced into the capillary by the enhanced EOF in the low ionic strength SM (Figure 1b). As the analytes migrate toward the cathode, the EOF velocity becomes slower and the electric field strength in the BGS becomes higher (Figure 4-1c). When almost all the SM in the capillary is removed out from the cathodic capillary end, the electrophoretic velocity of the analytes exceeds the EOF rate, resulting in the inversion of the sample migration direction (Figure 4-1d). After the complete removal of the SM, the analytes are separated by CDCZE/CDECK/CDMEKC during the anodic migration (Figure 4-1e).

In the LVSEP analysis, the inversion position of the concentrated analytes is significant for the separation performance [23]. To estimate the effects of the difference in the separation mode from normal CZE employed in the previous studies, the inversion position is theoretically considered. In the CDCZE/CDEKC analysis, the effective electrophoretic velocity in the BGS ($v_{\mathrm{ep,eff,BGS}}$) is expressed as follows [27]:

$$\begin{aligned} v_{\mathrm{ep,eff,BGS}} &= \left(\frac{1}{(K_{\mathrm{b}}[\mathrm{CD}]+1)} \mu_{\mathrm{ep,free}} + \frac{K_{\mathrm{b}}}{(K_{\mathrm{b}}[\mathrm{CD}]+1)} \mu_{\mathrm{ep,complex}} \right) \frac{V}{L} \\ &= \mu_{\mathrm{ep,eff,BGS}} \frac{V}{L} \end{aligned} \quad (1)$$

where $\mu_{ep,free}$, $\mu_{ep,complex}$, $\mu_{ep,eff,BGS}$, K_b, [CD], L, V are the electrophoretic mobilities of the free analyte and the analyte-CD complex, effective electrophoretic mobility of the analyte in the BGS, binding constant of the analyte with CD, the concentration of CD, whole capillary length, and applied voltage, respectively. From Eq. (1), we theoretically calculated the band width (w) and inversion position of the concentrated analyte from the inlet capillary end ($x_{sc,i}$) in the same way discussed in the previous paper [23]. The detailed calculation process is shown in the Supporting Information. The estimated results are expressed as follows.

$$w = -\frac{\mu_{ep,eff,BGS} L}{\gamma \mu_{EOF,SM}} \ln\left(-\frac{e\mu_{EOF,SM}}{\mu_{ep,free}}\right) \quad \text{(when } \mu_{EOF,SM} > -\mu_{ep,free}\text{)} \quad (2-1)$$

$$w = -\frac{\mu_{ep,eff,BGS}}{\mu_{ep,free}} \frac{L}{\gamma} \quad \text{(when } \mu_{EOF,SM} \leq -\mu_{ep,free}\text{)} \quad (2-2)$$

$$x_{sc,i} = -\frac{\mu_{ep,eff,BGS} L}{\gamma \mu_{EOF,SM}} \ln \gamma \quad \text{(when } \mu_{EOF,SM} > -\mu_{ep,free}\text{)} \quad (3-1)$$

$$x_{sc,i} = -\frac{\mu_{ep,eff,BGS} L}{\gamma \mu_{EOF,SM}} \ln\left(-\frac{e\gamma\mu_{EOF,SM}}{\mu_{ep,free}}\right) - \frac{\mu_{ep,eff,BGS}}{\mu_{ep,free}} \frac{L}{\gamma} \quad \text{(when } \mu_{EOF,SM} \leq -\mu_{ep,free}\text{)} \quad (3-2)$$

where $\mu_{EOF,SM}$, γ, and e are the electroosmotic mobility in the SM, conductivity ratio between the SM and the BGS, and base of the natural logarithm, respectively. It should be noted that all the estimated values are changed from those previously reported by the factor of $\mu_{ep,eff,BGS}/\mu_{ep,free}$. In the case of CDMEKC with more complicated interactions between the micelle, CD, and analytes, the same consideration can also be carried out because not the complicated interactions but only the obtained value of $\mu_{ep,eff,BGS}$ is important in our calculation.

In terms of w, it becomes narrower if the ratio $\mu_{ep,eff,BGS}/\mu_{ep,free}$ is smaller than unity,

which means that the analytes are more sharply focused. To our knowledge, however, w mainly depends on the molecular diffusion in the separation step [23], so that the effect of $\mu_{ep,eff,BGS}/\mu_{ep,free}$ will be limited.

In terms of $x_{sc,i}$, the theoretical calculation was carried out on the basis of Eq. (3–1). In LVSEP using a PVA-coated capillary, typical $\mu_{EOF,SM}$ of 5.0×10^{-4} $cm^2v^{-1}s^{-1}$ is usually larger than $\mu_{ep,free}$ of most anionic analytes so that Eq. (3–1) should be applied. The calculation was performed in the case of the typical LVSEP conditions, $\mu_{ep,free}$ = -1.0×10^{-4} $cm^2V^{-1}s^{-1}$ and $\mu_{EOF,SM} = 5.0 \times 10^{-4}$ $cm^2V^{-1}s^{-1}$. The estimated inversion positions of the concentrated analytes from the anodic capillary end are summarized in Table 1. The inversion position shifts toward the cathode if the ratio $\mu_{ep,eff,BGS}/\mu_{ep,free}$ is smaller than unity, which means that longer part of the capillary can be used for the effective separation. In the chiral analysis of anionic analytes, CDCZE with neutral chiral selectors or CDEKC with cationic chiral selectors are often employed, because the reduction in the electrophoretic mobility extends the separation window. Hence, $\mu_{ep,eff,BGS}/\mu_{ep,free}$ is often smaller than unity, where more efficient sample concentration and separation with more than 99% effective separation length are expected as shown in Table 1. In CDMEKC, on the other hand, the analytes interact with the fast migrating surfactant so that $\mu_{ep,eff,BGS}/\mu_{ep,free}$ tends to be more than unity. In this case, the inversion position moves toward the anode especially with small γ, causing less effective separation. As shown in Table 1, however, the effective separation length was estimated to be more than 93.74% indicating the loss of separation length will not be so significant. In general, loss of effective separation length would be more minimized by reducing the salt concentration of the SM and by making the conductivity of the BGS high to provide enough large γ.

LVSEP-CDCZE of Warfarin

The most fundamental enantioseparation mode, CDCZE using neutral CD was coupled with LVSEP. To compare the separation performance with that of the conventional analysis, the same experimental conditions were employed such as the capillary length, applied voltage, and BGS composition, except for the sample concentration and sample matrix. The same strategy was also applied to the CDEKC and CDMEKC analyses in this study.

In the CDCZE analysis, warfarin was analyzed as a model analyte employing 10 mM DM-β-CD as a neutral chiral selector in 25 mM MES buffer (pH 6.0), in accordance with the previous paper [28,29]. In the conventional CDCZE analysis, 50 ppm warfarin was well optically separated (Figure 2a) with the resolution of 2.5 (Table 2). In the LVSEP-CDCZE analysis, on the other hand, even 100 ppb racemic warfarin could be detected with the resolution of 2.6 (Figure 2b), where the sensitivity enhancement factor (SEF) was estimated to be 1,000. Since the noise level in LVSEP-CDCZE was similar to that in conventional CDCZE, the SEF was simply calculated from the following equation:

$$\mathrm{SEF} = \frac{h_{\mathrm{LVSEP}}}{h_{\mathrm{Conventional}}} \times \frac{C_{\mathrm{Conventional}}}{C_{\mathrm{LVSEP}}} \quad (4)$$

where, h and C are the peak height and sample concentration, respectively. The relative standard deviations (RSDs, n = 3) of the detection time, peak height, and peak area in LVSEP-CDCZE were estimated as 2.0%, 2.1%, and 5.8%, respectively, whereas those in the conventional CDCZE were 1.6%, 12%, and 17%, respectively.

In the CDCZE analyses, the anionic analytes form complexes with the neutral CD. Since the number of total negative charges is not changed in the complex formation but

the size is increased compared with the free analytes, the charge to size ratio of the complex is decreased, causing the reduction in the electrophoretic mobility. In the LVSEP-CDCZE analysis of warfarin, $\mu_{ep,eff,BGS}/\mu_{ep,free}$ was theoretically evaluated as 0.76 and 0.81 for first- and second migrating enantiomer, respectively, at γ = 500 . The maintained effective separation length was theoretically calculated to be more than 99.8% (see Supporting Information). As with the previous report [22], the effective separation length in LVSEP-CDCZE was experimentally estimated by subtracting the migration time (t_M) with the time of the drastic current change (t_i). As shown in Figure 2, t_M in conventional CDCZE was 15.5 min, whereas ($t_M - t_i$) in LVSEP-CDCZE was 15.7 min. These almost identical separation times gave the comparable resolutions, 2.5 and 2.6 obtained with Figure 2a and 2b, respectively. The effective separation length of 101% of the inlet-to-detector length estimated from $(t_{M,LVSEP} - t_i)/t_{M,CDCZE}$ agreed well with the theoretically calculated length of 99.8%.

LVSEP-CDEKC of Abscisic Acid

CDEKC using a charged CD was combined with LVSEP for analyzing a plant hormone, abscisic acid, as a model analyte. We employed 1.5 mM quaternary-β-CD as a charged chiral selector dissolved in 20 mM MES buffer (pH 6.0), as shown in the previous paper [29]. In the conventional CDEKC analysis, 250 ppm racemic abscisic acid was well separated (Figure 3a) with the resolution of 5.0 (Table 2). In the LVSEP-CDEKC analysis, even 100 ppb racemic abscisic acid could be detected with the resolution of 4.5 (Figure 3b), where the SEF was estimated as 800. The RSDs (n = 3) of the detection time, peak height, and peak area in LVSEP-CDEKC were estimated as 1.3%, 4.4%, and 4.6%, respectively, whereas those in the conventional CDCZE were

0.1%, 4.0%, and 3.5%, respectively.

The difference in the detection times of conventional CDEKC and LVSEP-CDEKC was found to be larger than that in CDCZE, which was mainly caused by the slow matrix removal. In CDEKC, we employed the longer capillary with the total/effective lengths of 60/50 cm than that of CDCZE with the lengths of 40/30 cm, but the applied voltage of –30 kV was the same in both cases. From the EOF rate in LVSEP-CDCZE, the time required for the matrix removal in LVSEP-CDEKC was calculated to be 5.5 min. However, the actual time (t_i) of 7.5 min was longer than that expected, indicating the reduction in the negative zeta potential of the inner capillary surface, where QA-β-CD might be adsorbed. Since the zeta potential of the PVA-coated capillary is fundamentally quite small, even a slight change in the surface condition tends to cause the drastic change in the enhanced EOF rate.

In the CDEKC analyses, the anionic analytes form complexes with the cationic CD, where the number of total negative charges is reduced in the complex formation and the size is increased compared with the free analytes. Hence the decrease in the charge to size ratio of the complex causes the reduction in the electrophoretic mobility as in CDCZE. The ratios of $\mu_{ep,eff,BGS}/\mu_{ep,free}$ (0.56 and 0.59) are smaller than unity, supporting that the separation ability was maintained in the LVSEP-CDEKC analysis.

LVSEP-CDMEKC of FITC-labeled Amino Acids

Amino acids are very important analytical targets in biological analysis, because they are related with many biological functions such as the protein metabolism, glucose metabolism, and neural transmission. Recently, the importance of D-amino acids has been recognized since they are found to be increased or decreased in a human body

suffering from several diseases in brain, kidney, and liver [2]. Hence, the chiral analysis of small amount of amino acids with high sensitivity and high resolution is required. Here, the combination of the LVSEP concentration, high resolution of the CDMEKC separation, and the high sensitive LIF detection was investigated to achieve the high performance chiral analyses.

CDMEKC employing SDS and neutral CD were combined with LVSEP. In the CDMEKC analysis, arginine (Arg), methionine (Met), and leucine (Leu) derivatized with FITC were analyzed as model analytes by employing 30 mM SDS and 10 mM γ-CD as the chiral selector in 40 mM borate buffer (pH 9.5), in accordance with the previous paper [24]. In the conventional CDMEKC analysis, 100 nM amino acids were optically resolved (Figure 4a). The resolutions were estimated as 5.1, 5.7, and 6.0 for Arg, Met, and Leu, respectively (Table 2). In the LVSEP-CDMEKC analysis, even 100 pM amino acids could be detected with the resolution of 4.2, 5.5, and 6.0 for Arg, Met, and Leu, respectively (Figure 4b). The SEFs were estimated as 1000, 1100, and 1300 for Arg, Met, and Leu, respectively. Opposite to LVSEP-CDEKC, t_i of 2.9 min was much smaller than that expected from LVSEP-CDCZE, probably because the slight adsorption of anionic SDS increased the negative zeta potential of the inner surface of the capillary.

Since the electrophoretic mobility of the FITC-labeled amino acids are increased by the interaction with the SDS micelle, the ratio $\mu_{ep,eff,BGS}/\mu_{ep,free}$ is larger than unity especially for earlier detected analytes, which might cause the slight band broadening and the reduction in the peak-to-peak distance. Typical reduction in resolution for the first detected Arg with the largest $\mu_{ep,eff,BGS}$ supported our theoretical consideration. Anyway, the optical resolutions were almost kept up as that in LVSEP-CDCZE/CDEKC,

indicating the effect of $\mu_{ep,eff,BGS}$ on the preconcentration is often limited. These good results demonstrated the versatile applicability of LVSEP to many separation modes.

It should be emphasized again in LVSEP-CDCZE/CDEKC/CDMEKC that the sample filled in the whole capillary, which is theoretically the maximum injection volume by pressure, could be well concentrated and separated without much loss of the effective separation length. Thus, it is not necessary to optimize the sample injection volume in the LVSEP analysis. This is one of the most invaluable advantages of LVSEP coupled with any separation modes in CE.

EE Assay of Ibuprofen

Quantification of a minor enantiomer from the excessive amount of the major enantiomer is one of the most important issues in the chiral analysis. However, the large peak of the excess amount of the enantiomer often overlaps the other peak, making the quantitative EE assay difficult. If the conventional online concentration techniques were applied to the EE assay, the reduction in optical resolution would make the chiral separation more difficult, resulting in poor EE quantification. On the other hand, one of the most significant advantages of LVSEP is the capability of maintaining the separation performance, so that the comparable enantioseparation and quantification with a conventional mode is expected to be provided. Hence, the EE assay was performed to verify the compatibility of LVSEP with the chiral analysis.

As a typical assay of 99% EE, the mixture of 99.5% (S)-ibuprofen with 0.5% (R)-ibuprofen was analyzed both by conventional CDCZE and by LVSEP-CDCZE using TM-β-CD as a chiral selector [30]. In LVSEP-CDCZE, 2 ppm (S)-ibuprofen and 10 ppb (R)-ibuprofen were well separated with the resolution of 4.7 (Figure 5b),

whereas 1000 ppm (S)-ibuprofen and 5 ppb (R)-ibuprofen were resolved with the resolution of 4.8 (Figure 5a). The SEF was evaluated as 500 for both enantiomers, and the limits of detection (LODs) (S/N = 3) in LVSEP-CDCZE were estimated to be 3.7 ppb and 4.7 ppb for (R)- and (S) ibuprofen, respectively. For quantitative analysis of enantiomers, the peak areas must be corrected with the factor of v_s [31], which is the sample velocity at the detection point. In the conventional CDCZE analysis, the electrophoretic mobility is proportional to $1/t_M$, where t_M is the detection time of the analyte, so that the area can easily be corrected with the factor of $1/t_M$. In LVSEP-CDCZE, on the other hand, $1/t_M$ is not proportional to v_s because t_M includes the time of the LVSEP concentration process. Since the time of the LVSEP concentration can be estimated from t_i [22], t_M was corrected by subtracting with t_i in this study for the EE quantification. As a result, EE was estimated as 99.05% ± 0.048% (n = 4) in LVSEP-CDCZE and 99.11% ± 0.082% (n = 4) in conventional CDCZE, indicating that good chiral quantification performance of CDCZE was maintained even after applying LVSEP. Moreover, the author also succeeded in the assays of the EE ratio up to 99.60%, where 5 ppm (S)-ibuprofen and 10 ppb (R)-ibuprofen were analyzed by LVSEP-CDCZE. In conventional CDCZE, on the other hand, such higher EE ratio could not be determined because the required concentration of (S)-ibuprofen, 2,500 ppm, was too high to be dissolved in the BGS. Hence, LVSEP-CDCZE is also suitable for the assay of the high EE ratio.

Analysis of Ibuprofen in Urine Sample

Some of the most important targets of the chiral analysis are drug components in biological fluids such as blood, saliva, and urine. Since these fluids contain many salts

which directly interfere with the LVSEP preconcentration process, purification such as gel filtration [22], liquid phase microextraction (LPME) [32], and SPE [33] are required in the LVSEP-CDCZE analysis. Taking into account of the molecular size of the analytes, LPME and SPE are suitable in this study. In LPME-LVSEP, however, the EOF velocity would become too slow in the preconcentration stage due to the combination of the PVA-coated capillary and a hydrophobic solvent. Thus, SPE-LVSEP with a C_{18} column was employed in this study. The conductivity of the reconstituted sample solution was reduced to 10 μS/cm from 20 mS/cm in the original urine sample. As shown in the previous report [22], the LVSEP analysis could be performed without dilution when the conductivity of the sample solution is less than 100 μS/cm. Hence, the desalting performance of the SPE is sufficient for the LVSEP concentration.

Urine sample containing 500 ppb racemic ibuprofen after the SPE purification was analyzed in the same LVSEP conditions as discussed in the previous section on the EE assay. As a typical result, racemic ibuprofen was well detected and optically separated with the resolution of 5.1 as shown in Figure 6a. By the calibration curve determined from the analysis of ibuprofen spiked in the blank urine sample with the SPE purification, the recovery rate was estimated as 84.0% for (S)-ibuprofen and 86.6% for (R)-ibuprofen. The similar results were obtained in the sample concentration ranging from 25 ppb to 4.0 ppm, where the limits of quantification (LOQs) (S/N = 10) were estimated as 14 ppb and 17 ppb for (R)- and (S)-ibuprofen, respectively. Compared with the LOQs of 500 ppb and 250 ppb in previous reports using SPE-CDCZE [34] and SPE-HPLC [35], respectively, the better sensitivity in this study indicated the practical utility of SPE-LVSEP-CDCZE. Thus, sufficient desalting was achieved for the successful analysis of urine sample by LVSEP-CDCZE. Further improvement of the

analytical performance for several important analytes with more optimized recovery is expected to be realized soon by the combination of LVSEP with the SPE preconcentration.

Conclusions

The effects of the chiral selectors on the LVSEP performance were investigated both theoretically and experimentally. We demonstrated that the excellent preconcentration efficiency up to 1,300-fold sensitivity increases was achieved with maintaining similar optical resolutions. The EE assay of up to 99.6% was also carried out without loss of analytical performance by LVSEP-CDCZE. Finally, the combination of the sample purification by using the C_{18} SPE column with LVSEP-CDCZE was shown to be useful for the analyses of the real sample containing many unnecessary salts. Therefore, the application of the easy operating and high performance LVSEP to the chiral analysis will contribute in many areas such as biology, chemistry, medicine, and pharmaceutics.

Acknowledgment

T. K. thanks the support from the research fellowships of the Japan Society for Promotion of Science (JSPS) for young scientists. This development was supported in part by SENTAN, JST. This research was supported in part by the Global COE Program “Integrated Materials Science (#B-09)” of the Ministry of Education, Culture, Sports, Science and Technology, Japan, administrated by JSPS.

References

[1] A. J. Hutt, J. O'Grady, J. Antimicrob. Chemother. 37 (1996) 7.

[2] K. Hamase, A. Morikawa, K. Zaitsu, J. Chromatogr. B 781 (2002) 73.

[3] K. Mori, Bioorg. Med. Chem. 15 (2007) 7505.

[4] F. Kitagawa, K. Otsuka, J. Chromatogr. B in press.

[5] S. Fanali, J. Chromatogr. A 875 (2000) 89.

[6] G.. Blaschke, B. Chankvetadz, J. Chromatogr. A 906 (2001) 309.

[7] C. García-Ruiz, M. L. Marina, Electrophoresis 27 (2006) 195.

[8] L. Sánchez-Hernández, A. L. Crego, M. L. Marina, C. García-Ruiz, Electrophoresis 29 (2008) 237.

[9] L. Sánchez-Hernández, C. García-Ruiz, M. L. Marina, A. L. Crego, Electrophoresis 31 (2010) 28.

[10] D.S. Burgi, R.-L. Chien, Anal. Biochem. 202 (1992) 306.

[11] J.P. Quirino, S. Terabe, Anal. Chem. 71 (1999) 1638.

[12] J. P. Quirino, S. Terabe, K. Otsuka, J. B. Vincent, G. Vigh, J. Chromatogr. A 838 (1999) 3.

[13] S. Kodama, A. Yamamoto, A Matsunaga, T. Soga, K. Minoura, J. Chromatogr. A 875 (2000) 371.

[14] F. Wang, M. G. Khaledi, J. Chromatogr. B Biomed. Sci. Appl. 731 (1999) 187.

[15] J.-Z. Song, J. Chen, S.-J. Tian, Z.-P. Sun, J. Pharm. Biomed. Anal. 21 (1999) 569.

[16] Z. Wang, C. Liu, J. Kang, J. Chromatogr. A 1218 (2011) 1775.

[17] J. P. Quirino, S. Terabe, Science 282 (1998) 465.

[18] A.R. Timerbaev, T. Hirokawa, Electrophoresis 27 (2006) 323.

[19] P. Britz-McKibbin, D.D.Y. Chen, Anal. Chem. 72 (2000) 1242.

[20] K. Sueyoshi, K. Hashiba, T. Kawai, F. Kitagawa, K. Otsuka, Electrophoresis 32 (2011) 1233.

[21] Y. He, H.K. Lee, Anal. Chem. 71 (1999) 995.

[22] T. Kawai, M. Watanabe, K. Sueyoshi, F. Kitagawa, K. Otsuka, J. Chromatogr. A in press.

[23] T. Kawai, K. Sueyoshi, F. Kitagawa, K. Otsuka, Anal. Chem. 82 (2010) 6504.

[24] L. J. Jin, I. Rodriguez, S. F. Y. Li, Electrophoresis 20 (1999) 1538.

[25] M. Gllges, M.H. Kleemlss, G. Schomburg, Anal. Chem. 66 (1994) 2038.

[26] Y. Okamoto, F. Kitagawa, K. Otsuka, Anal. Chem. 79 (2007) 3041.

[27] Y. Tanaka, M. Yanagawa, S. Terabe, J. High Resol. Chromatogr. 19 (1996) 421.

[28] M. Ufer, B. Kammerer, J. Kirchheiner, A. Rane, J.-O. Svensson, J. Chromatogr. B 809 (2004) 217.

[29] Y. Tanaka, S. Terabe, J. Chromatogr. A 781 (1997) 151.

[30] M. Blance, J. Coello, H. Iturriaga, S. Maspoch, C. Perez-Maseda, J. Chromatogr. A 793 (1998) 165.

[31] L. G. Blomberg, H. Wan, Electrophoresis 21 (2000) 1940.

[32] K. Choi, Y. G. Jin, D. S. Chung, J. Chromatogr. A 1216 (2009) 6466.

[33] A. Macià, F. Borrull, C. Aguilar, M. Calull, Electrophoresis 24 (2003) 2779.

[34] F. K. Główka, M. Karaźniewicz, Anal. Chim. Acta 540 (2005) 95.

[35] A. R. M. Oliveira, E. J. Cesarino, P. S. Bonato, J. Chromatogr. B 818 (2005) 285.

Figure Legends

Figure 1. Concept of LVSEP-CDCZE/CDEKC/CDMEKC in the PVA-coated capillary. v_{ep}, v_{EOF} and v_s mean the electrophoretic velocity of the analyte, the EOF velocity, and apparent velocity of the analyte, respectively.

Figure 2. Electropherograms of warfarin obtained in (a) conventional CDCZE and (b) LVSEP-CDCZE. Sample concentration, (a) 50 ppm and (b) 100 ppb; UV detection, 200 nm. The broken line represents the current change in LVSEP-CDCZE.

Figure 3. Enantioseparations of racemic abscisic acid by (a) conventional CDEKC and (b) LVSEP-CDEKC. Sample concentration, (a) 250 ppm and (b) 100 ppb; UV detection, 250 nm.

Figure 4. Enantioseparations of FITC-labeled amino acids in (a) conventional CDMEKC and (b) LVSEP-CDMEKC. Sample concentration, (a) 100 nM and (b) 100 pM; LIF detection, $\lambda_{ex}/\lambda_{em}$ of 488/520 nm.

Figure 5. EE assay of ibuprofen in (a) conventional CDCZE and (b) LVSEP-CDCZE. Sample concentration, (a) 1000 ppm (S)-ibuprofen and 5 ppm (R)-ibuprofen; (b) 2 ppm (S)-ibuprofen and 10 ppb (R)-ibuprofen. UV detection, 200 nm.

Figure 6. LVSEP-CDCZE of purified ibuprofen from the urine sample. The original concentrations of ibuprofen in the urine, (a) 500 ppb and (b) 0 ppb (blank); UV detection, 200 nm.

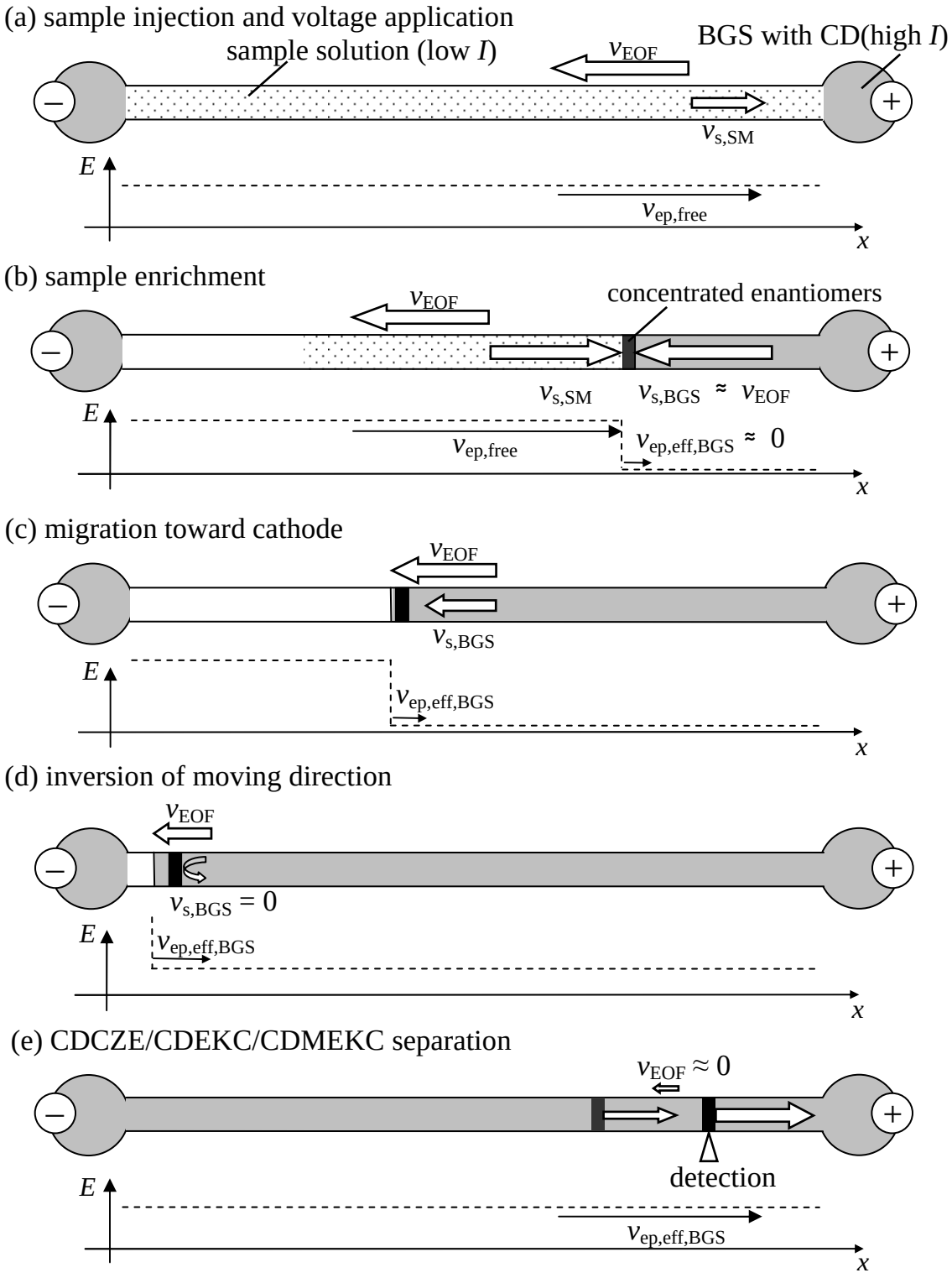

Figure 1. Concept of LVSEP-CDCZE/CDEKC/CDMEKC in the PVA-coated capillary. v_{ep}, v_{EOF} and v_s mean the electrophoretic velocity of the analyte, the EOF velocity, and apparent velocity of the analyte, respectively.

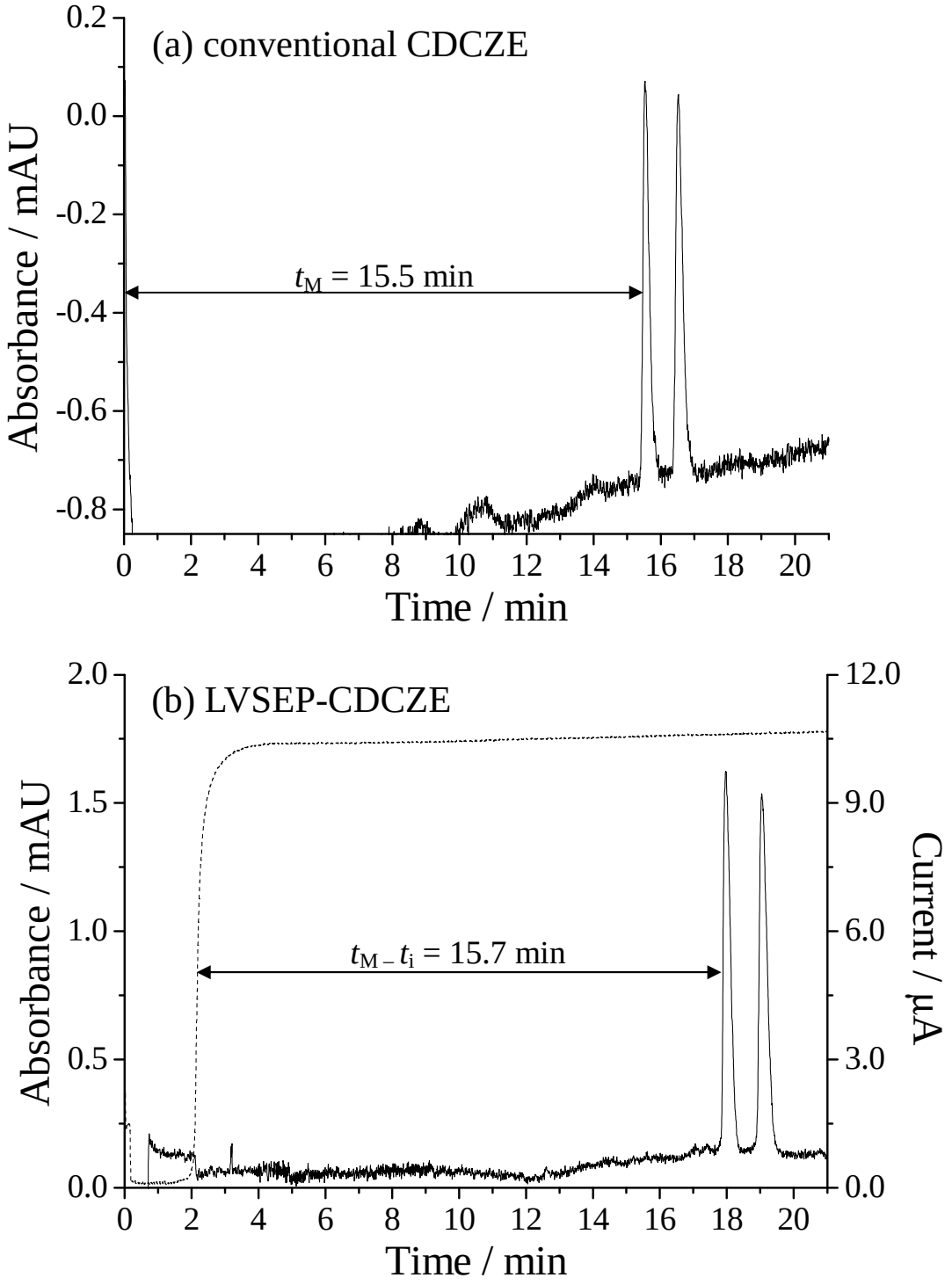

1 **Figure 2.** Electropherograms of warfarin obtained in (a) conventional CDCZE and (b)
2 LVSEP-CDCZE. Sample concentration, (a) 50 ppm and (b) 100 ppb; UV detection, 200
3 nm. The broken line represents the current change in LVSEP-CDCZE.

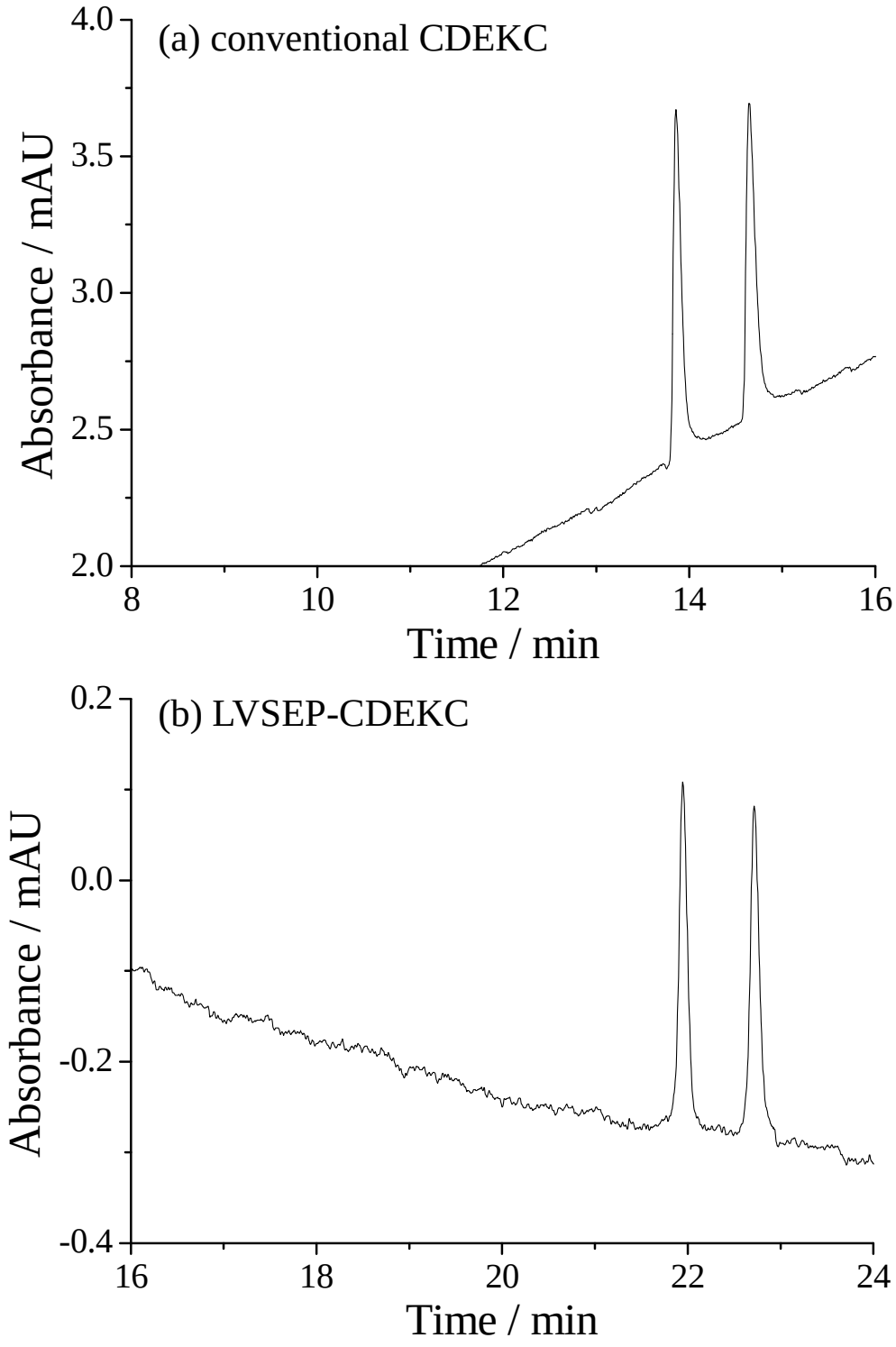

Figure 3. Enantioseparation of racemic abscisic acid by (a) conventional CDEKC and (b) LVSEP-CDEKC. Sample concentration, (a) 250 ppm and (b) 100 ppb; UV detection, 250 nm.

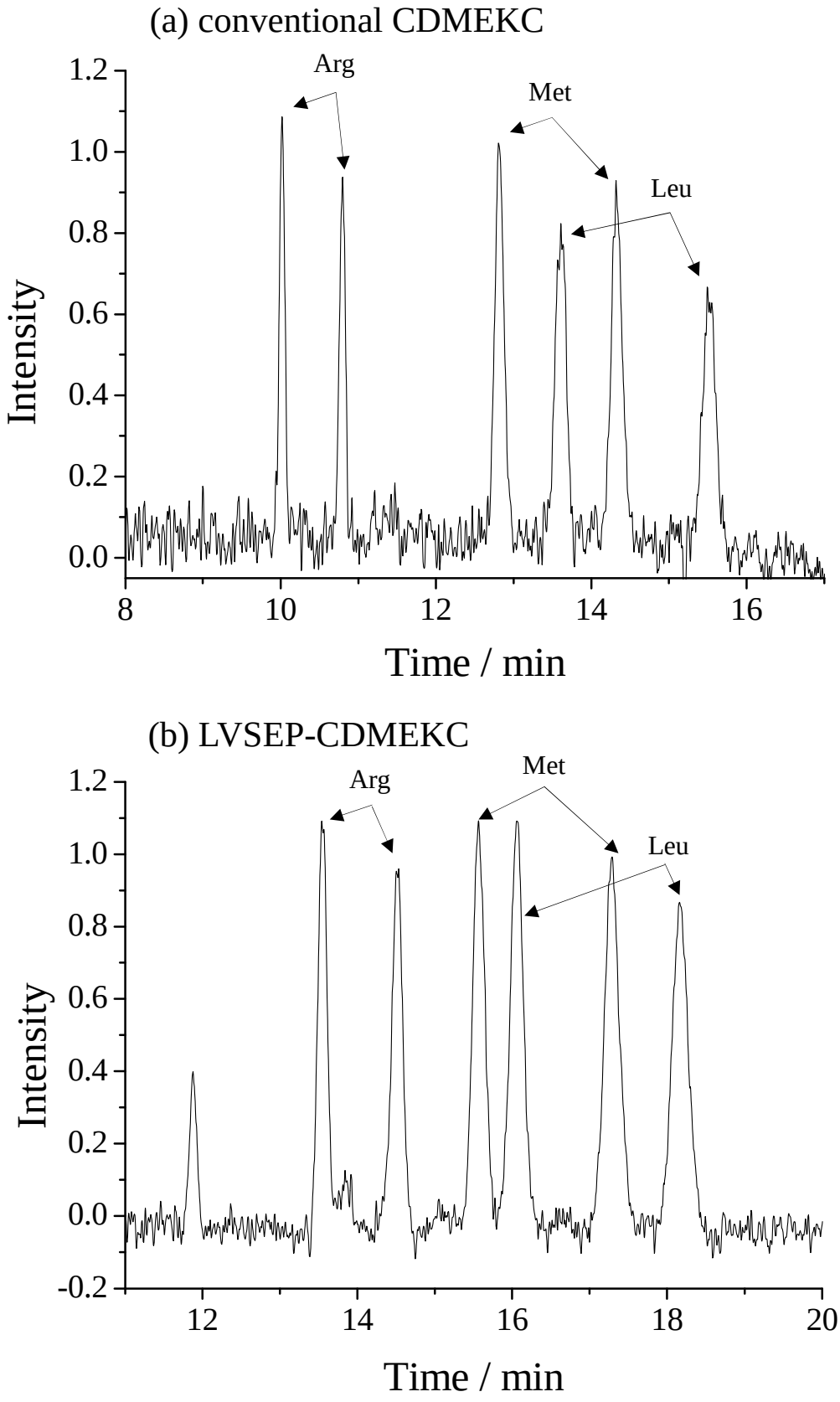

Figure 4. Enantioseparation of FITC-labeled amino acids in (a) conventional CDMEKC and (b) LVSEP-CDMEKC. Sample concentration, (a) 100 nM and (b) 100 pM; LIF detection, $\lambda_{ex}/\lambda_{em}$ of 488/520 nm.

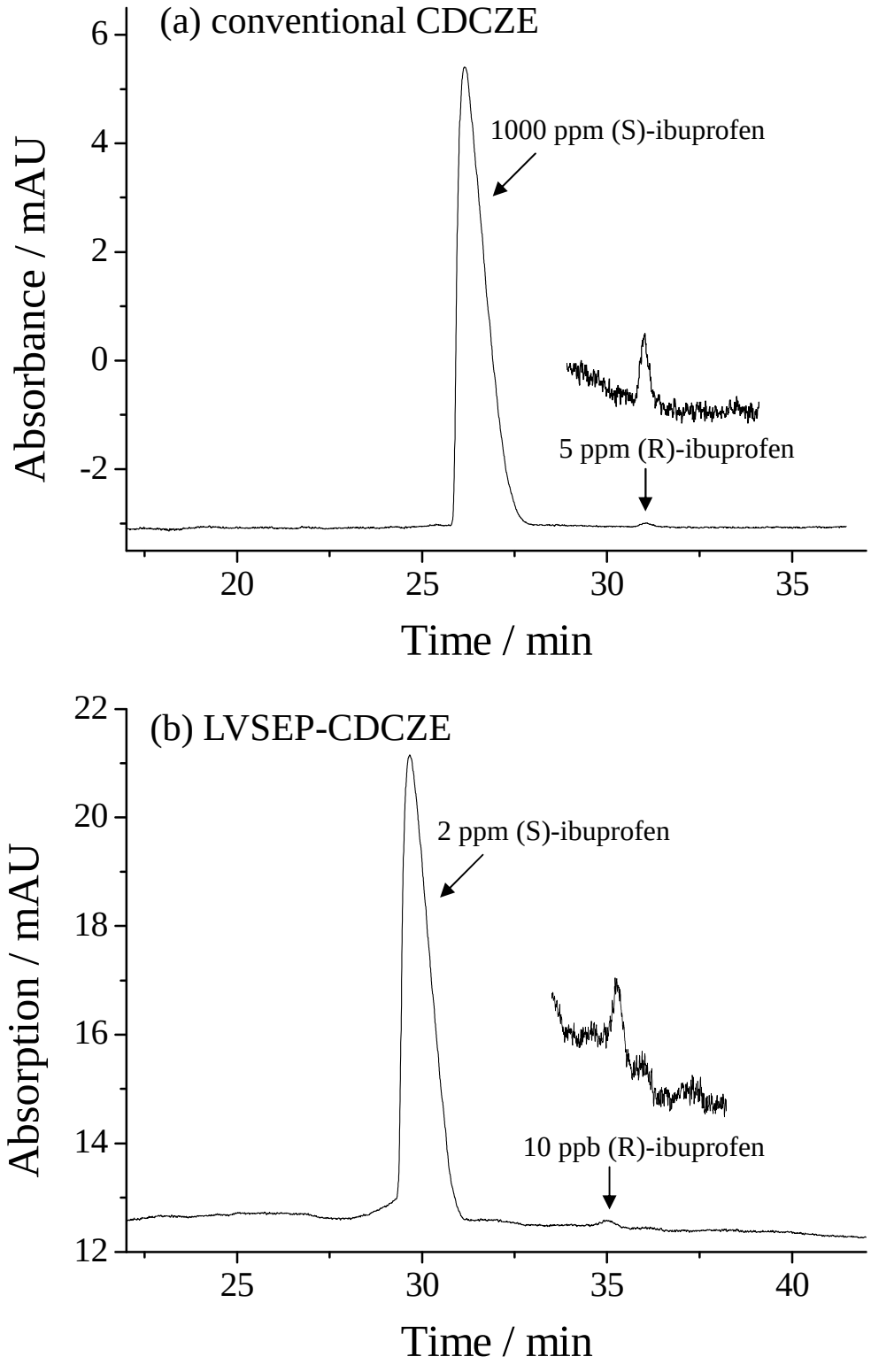

Figure 5. EE assay of ibuprofen in (a) conventional CDCZE and (b) LVSEP-CDCZE. Sample concentration, (a) 1000 ppm (S)-ibuprofen and 5 ppm (R)-ibuprofen; (b) 2 ppm (S)-ibuprofen and 10 ppb (R)-ibuprofen. UV detection, 200 nm.

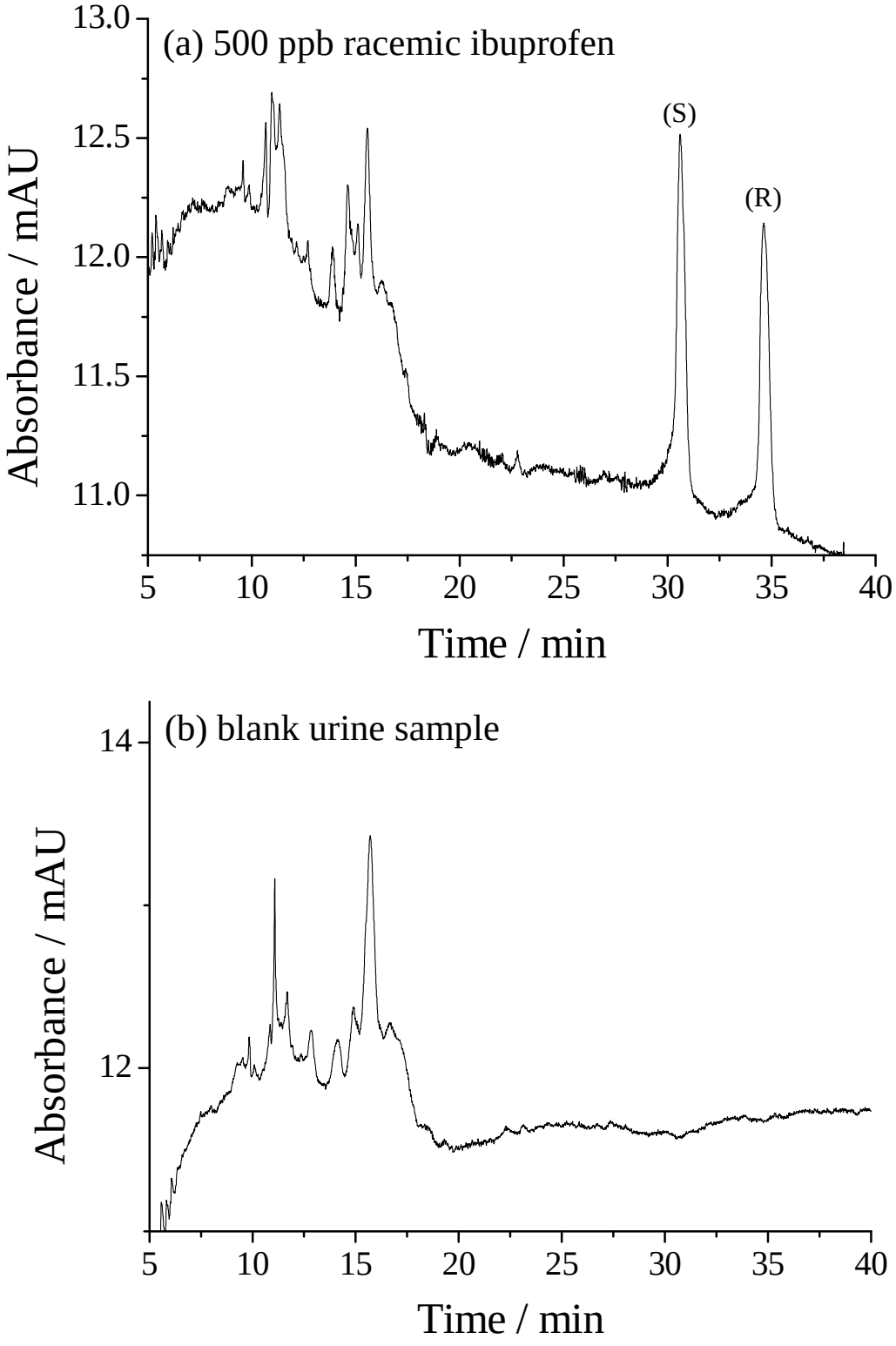

Figure 6. LVSEP-CDCZE of purified ibuprofen from the urine sample. The original concentrations of ibuprofen in the urine, (a) 500 ppb and (b) 0 ppb (blank); UV detection, 200 nm.

Table 1. Theoretical estimation of the inversion position of the concentrated analytes from the anodic capillary end.

$\mu_{ep,eff,BGS}/\mu_{ep,free}$	γ				
	50	100	200	500	1,000
0.25	99.61	99.77	99.87	99.94	99.97
0.5	99.22	99.54	99.74	99.88	99.93
1	98.44	99.08	99.47	99.75	99.86
2	96.87	98.16	98.94	99.50	99.72
4	93.74	96.32	97.88	99.01	99.45

Calculation condition, $\mu_{ep,free} = -1.0 \times 10^{-4}$ $cm^2V^{-1}s^{-1}$ and $\mu_{EOF,SM} = 5.0 \times 10^{-4}$ $cm^2V^{-1}s^{-1}$. Expressed as %ratio of the whole capillary length.

Table 2. Summary of the separation mode, employed BGS composition, obtained resolution, and SEF for each analyte.

analyte	separation mode	BGS composition	σ_{BGS} / mS/cm	R_s (normal / LVSEP)	SEF
warfarin	CDCZE	10 mM DM-β-CD, 25 mM MES buffer (pH 6.0)	0.54	2.5 / 2.6	1,000
ibuprofen	CDCZE	40 mM TM-β-CD, 25 mM MES buffer (pH 6.0)	0.54	6.7 / 6.9	500
abscisic acid	CDEKC	1.5 mM quaternary-β-CD, 20 mM MES buffer (pH 6.0)	1.43	5.0 / 4.5	800
FITC-Arg	CDMEKC	30 mM SDS, 10 mM γ-CD, 40 mM borate buffer (pH 9.5)	2.70	5.1 / 4.2	1,000
FITC-Met				5.7 / 5.5	1,100
FITC-Leu				6.0 / 6.0	1,300

Supporting information

Jan 27, 2012

Highly Sensitive Chiral Analysis in Capillary Electrophoresis with Large-volume Sample Stacking with an Electroosmotic Flow Pump

Takayuki Kawai*, Hiroshi Koino, Kenji Sueyoshi, Fumihiko Kitagawa, and Koji Otsuka

7 pages

Calculation of the inversion position of the concentrated analytes

In the main text, detailed calculations from Eq. (1) to Eqs. (2) and (3) are skipped to be easily understandable. In this supporting section, the complicated calculations are proposed to obtain w and $x_{sc,i}$. Although the main stream of the calculation process is almost the same as that in our previous report, the effect of adding CD into the electrolyte was discussed in detail.

At first, we defined many parameters, x_b, x_{sa}, x_{sc}, E_{BGS}, E_{SM}, and so on as shown in Figure S1. The electroosmotic mobility in the PVA-coated capillary filled with the BGS ($\mu_{EOF,BGS}$) was less than 0.3×10^{-4} $cm^2V^{-1}s^{-1}$, so that $\mu_{EOF,BGS}$ was neglected in this study. As discussed in the previous report [18], fundamental parameters are calculated as Eqs. (S1)–(S4).

$$E_{SM} = \frac{\gamma V}{(\gamma-1)x_b + L} \tag{S1}$$

$$E_{BGS} = \frac{V}{(\gamma-1)x_b + L} \tag{S2}$$

$$v_{ep,BGS} = \frac{\mu_{ep} V}{(\gamma-1)x_b + L} \tag{S3}$$

$$v_{EOF} \approx \frac{\gamma \mu_{EOF,SM} V x_b}{\{(\gamma-1)x_b + L\}L} \tag{S4}$$

The SM/BGS boundary moves according to the EOF, x_b can be expressed as a function of t.

$$\begin{aligned} x_b &= L - \int_0^t \frac{\mu_{EOF,SM}\gamma V x_b}{\{(\gamma-1)x_b + L\}L} dt \\ &= L - \int_0^t \frac{\mu_{EOF,SM}\gamma V}{(\gamma-1)L} dt + \int_0^t \frac{\mu_{EOF,SM}\gamma V}{\{(\gamma-1)x_b + L\}(\gamma-1)} dt \\ &= L - \frac{\mu_{EOF,SM}\gamma V}{(\gamma-1)L} t + \int_0^t \frac{\mu_{EOF,SM}\gamma V}{\{(\gamma-1)x_b + L\}(\gamma-1)} dt \end{aligned} \tag{S4}$$

$$\int_0^t \frac{V}{\{(\gamma-1)x_b + L\}}dt = \frac{(\gamma-1)}{\gamma\mu_{EOF,SM}}\left\{x_b - L + \frac{\gamma\mu_{EOF,SM}V}{(\gamma-1)L}t\right\} \quad (S5)$$

If x_{sa} is the position of the anode-side end of the concentrated sample band as shown in Figure S1, (x_{sa}–x_b) is the length by which the analytes at the anode-side end migrate electrophoretically from the boundary. Therefore, (x_{sa}–x_b) can also be calculated by integrating $v_{ep,BGS}$ and expressed as a function of t.

$$x_{sa} - x_b = \int_0^t \frac{-\mu_{ep,eff,BGS}V}{(\gamma-1)x_b + L}dt \quad (S6)$$

Substitution of Eq. (S5) into Eq. (S6) gives the following equation.

$$\begin{aligned} x_{sa} - x_b &= \frac{-\mu_{ep,eff,BGS}(\gamma-1)}{\mu_{EOF,SM}\gamma}\left\{x_b - L + \frac{\mu_{EOF,SM}\gamma V}{(\gamma-1)L}t\right\} \\ &= -\frac{\mu_{ep,eff,BGS}V}{L}t + \frac{\mu_{ep,eff,BGS}(\gamma-1)}{\mu_{EOF,SM}\gamma}(L - x_b) \end{aligned} \quad (S7)$$

Here, by solving the differential equation of t and x,

$$x_b = L - \int_0^t \frac{\mu_{EOF,SM}\gamma V x_b}{\{(\gamma-1)x_b + L\}L}dt \quad (S8)$$

$$\frac{dx_b}{dt} = -\frac{\mu_{EOF,SM}\gamma V x_b}{\{(\gamma-1)x_b + L\}L} \quad (S9)$$

$$-\frac{\{(\gamma-1)x_b + L\}L}{\mu_{EOF,SM}\gamma V x_b}dx_b = dt \quad (S10)$$

$$\int -\left\{\frac{(\gamma-1)L}{\gamma\mu_{EOF,SM}V} + \frac{L^2}{\gamma\mu_{EOF,SM}V}\frac{1}{x_b}\right\}dx_b = \int dt \quad (S11)$$

From initial condition, x_b is equal to L when t = 0. Thus, Eq. (S11) is solved as

$$t = \frac{(\gamma-1)}{\gamma\mu_{EOF,SM}V}(L - x_b) + \frac{L^2}{\gamma\mu_{EOF,SM}V}\ln\left(\frac{L}{x_b}\right) \quad (S12)$$

By substituting Eq. (S12) into Eq. (S7), the term (x_{sa}–x_b) can be expressed as a function of x_b,

$$x_{sa} - x_b = \frac{-\mu_{ep,eff,BGS} L}{\gamma \mu_{EOF,SM}} \ln\left(\frac{L}{x_b}\right) \quad \text{(S13)}$$

Provided that x_b is $x_{b,B}$ when $v_{ep,free,SM}$ exceeds v_{EOF}, and that x_b is $x_{b,F}$ when the whole analytes are stacked out, $x_{b,F}$ can be given as follows.

i) If $\mu_{EOF,SM} > \mu_{ep,free}$, some of the analytes were flashed out from the cathodic end due to the fast EOF. After decreasing the length of the SM zone and increasing the electric field, the analyte can move against the EOF toward the anode. Hence, this balanced condition can be expressed as follows,

$$v_{EOF} = -v_{ep,free,SM} \quad \text{(S14–1)}$$

$$\frac{\gamma \mu_{EOF,SM} V x_{b,B}}{\{(\gamma-1)x_{b,B} + L\}L} = \frac{-\gamma \mu_{ep,free} V}{(\gamma-1)x_{b,B} + L} \quad \text{(S15–1)}$$

$$x_{b,B} = \frac{-\mu_{ep,free} L}{\mu_{EOF,SM}} \quad \text{(S16–1)}$$

Meanwhile, if $v_{ep,free,SM} > v_{EOF}$, the analyte at the cathodic end moves by the length of $x_{b,B}$ from $t = t_B$ to $t = t_F$. Therefore, $x_{b,B}$ can be also given by the following equation.

$$\begin{aligned} x_{b,B} &= \int_{t_B}^{t_F} \frac{-\gamma \mu_{ep,free} V}{(\gamma-1)x + L} dt \\ &= \int_{x_{b,B}}^{x_{b,F}} \frac{-\gamma \mu_{ep,free} V}{(\gamma-1)x_b + L} \cdot \frac{-\{(\gamma-1)x_b + L\}L}{\gamma \mu_{EOF,SM} V x_b} dx_b \\ &= \frac{\mu_{ep,free} L}{\mu_{EOF,SM}} \int_{x_B}^{x_F} \frac{dx_b}{x_b} \\ &= -\frac{\mu_{ep,free} L}{\mu_{EOF,SM}} \ln\left(\frac{x_{b,B}}{x_{b,F}}\right) \end{aligned} \quad \text{(S17)}$$

By solving Eqs. (S16–1) and (S17), $x_{b,F}$ is expressed by the Eq. (S19–1).

$$\ln\left(\frac{x_{b,B}}{x_{b,F}}\right) = 1 \quad \text{(S18–1)}$$

$$x_{b,F} = \frac{x_{b,B}}{e} = -\frac{\mu_{ep,free} L}{e\mu_{EOF,SM}} \quad \text{(S19–1)}$$

ii) If $\mu_{EOF,SM} \leq \mu_{ep,free}$, the analyte can migrate against the fast EOF immediately after the applying the voltage. Thus, $x_{b,B}$ is equal to L.

$$x_{b,B} = L \quad \text{(S16–2)}$$

As with Eq. (S15), L can be expressed as follows.

$$\begin{aligned} L &= \int_0^{t_F} \frac{-\gamma\mu_{ep,free} V}{(\gamma-1)x_b + L} dt \\ &= \int_L^{x_{b,F}} \frac{-\gamma\mu_{ep,free} V}{(\gamma-1)x_b + L} \cdot \frac{-\{(\gamma-1)x_b + L\}L}{\gamma\mu_{EOF,SM} V x_b} dx_b \\ &= \frac{\mu_{ep,free} L}{\mu_{EOF,SM}} \int_L^{x_{b,F}} \frac{dx_b}{x_b} \\ &= \frac{-\mu_{ep,free} L}{\mu_{EOF,SM}} \ln\left(\frac{L}{x_{b,F}}\right) \end{aligned} \quad \text{(S17–2)}$$

$$\ln\left(\frac{L}{x_{b,F}}\right) = -\frac{\mu_{EOF,SM}}{\mu_{ep,free}} \quad \text{(S18–2)}$$

$$x_{b,F} = L e^{\frac{\mu_{EOF,SM}}{\mu_{ep,free}}} \quad \text{(S19–2)}$$

Provided that ($x_{sa,F}$–$x_{b,F}$) is w, substitution of Eq. (S19) into (S13) gives w by the following equation.

(when $\mu_{EOF,SM} > -\mu_{ep,free}$) $$w = -\frac{\mu_{ep,eff,BGS} L}{\gamma\mu_{EOF,SM}} \ln\left(-\frac{e\mu_{EOF,SM}}{\mu_{ep,free}}\right) \quad \text{(S20–1)}$$

(when $\mu_{EOF,SM} \leq -\mu_{ep,free}$) $$w = -\frac{\mu_{ep,eff,BGS}}{\mu_{ep,free}} \frac{L}{\gamma} \quad \text{(S20–2)}$$

When the whole analytes are stacked out, the cathodic side of the concentrated band is just on the boundary. Therefore, w can be identified as the width of the concentrated

band.

When the concentrated analytes start to move against the EOF, the SM plug length remaining in the channel/capillary ($x_{b,i}$) is expressed by the following Eq. (S-22).

$$\frac{-\mu_{ep,eff,BGS}V}{(\gamma-1)x_{b,i}+L}=\frac{\mu_{EOF,SM}\gamma Vx_{b,i}}{\{(\gamma-1)x_{b,i}+L\}L} \tag{S21}$$

$$x_{b,i}=\frac{-\mu_{ep,eff,BGS}L}{\gamma\mu_{EOF,SM}} \tag{S22}$$

The distance between the cathodic end of the stacked analytes and the cathodic end of the channel/capillary (x_{sc}) is equal to ($x_{sa} - w$). From Eqs. (S13), (S20) and (S22), x_{sc} at the inversion time ($x_{sc,i}$) is given as follows.

(when $\mu_{EOF,SM} > -\mu_{ep,free}$)

$$\begin{aligned}x_{sc,i}&=-\frac{\mu_{ep,eff,BGS}L}{\gamma\mu_{EOF,SM}}-\frac{\mu_{ep,eff,BGS}L}{\gamma\mu_{EOF,SM}}\ln\left(-\frac{\gamma\mu_{EOF,SM}}{\mu_{ep,free}}\right)+\frac{\mu_{ep,eff,BGS}L}{\gamma\mu_{EOF,SM}}\ln\left(-\frac{e\mu_{EOF,SM}}{\mu_{ep,free}}\right)\\&=-\frac{\mu_{ep,eff,BGS}L}{\gamma\mu_{EOF,SM}}\ln\gamma\end{aligned} \tag{S23–1}$$

(when $\mu_{EOF,SM} \le -\mu_{ep,free}$)

$$\begin{aligned}x_{sc,i}&=-\frac{\mu_{ep,eff,BGS}L}{\gamma\mu_{EOF,SM}}-\frac{\mu_{ep,eff,BGS}L}{\gamma\mu_{EOF,SM}}\ln\left(-\frac{\gamma\mu_{EOF,SM}}{\mu_{ep,free}}\right)-\frac{\mu_{ep,eff,BGS}}{\mu_{ep,free}}\frac{L}{\gamma}\\&=-\frac{\mu_{ep,eff,BGS}L}{\gamma\mu_{EOF,SM}}\ln\left(-\frac{e\gamma\mu_{EOF,SM}}{\mu_{ep,free}}\right)-\frac{\mu_{ep,eff,BGS}}{\mu_{ep,free}}\frac{L}{\gamma}\end{aligned} \tag{S23–2}$$

Therefore, the effective separation length ($x_d - x_{sc,i}$) is estimated as follows:

(when $\mu_{EOF,SM} > -\mu_{ep,free}$)

$$x_d-x_{sc,i}=x_d+\frac{\mu_{ep,eff,BGS}L}{\gamma\mu_{EOF,SM}}\ln\gamma \tag{S24–1}$$

(when $\mu_{EOF,SM} \le -\mu_{ep,free}$)

$$x_{\mathrm{d}} - x_{\mathrm{sc,i}} = x_{\mathrm{d}} + \frac{\mu_{\mathrm{ep,eff,BGS}} L}{\gamma \mu_{\mathrm{EOF,SM}}} \ln\left(-\frac{e\gamma\mu_{\mathrm{EOF,SM}}}{\mu_{\mathrm{ep,free}}} \right) + \frac{\mu_{\mathrm{ep,eff,BGS}}}{\mu_{\mathrm{ep,free}}} \frac{L}{\gamma} \qquad \text{(S24–2)}$$

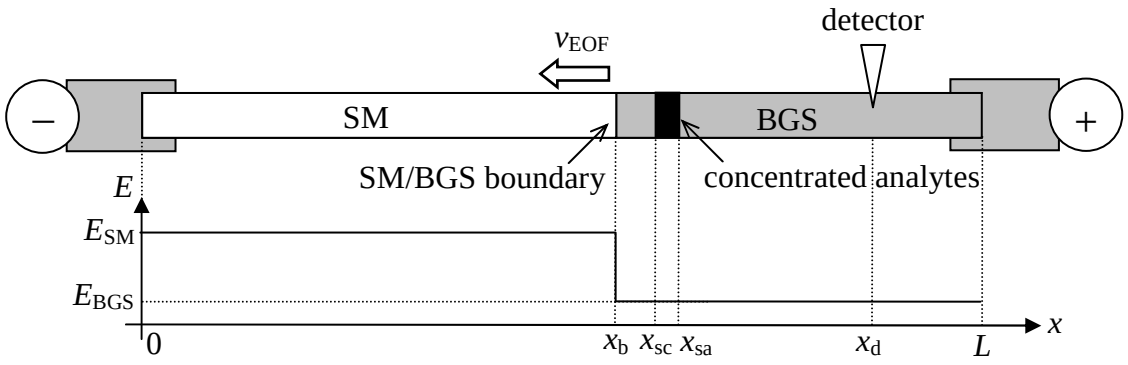

Fig. S1. Schematic representation for the parameters used in the theoretical model. *E* and *x* mean electric field and the position from the cathodic capillary end. All positions are expressed as the distance from the cathodic channel end. Subscripts b, sc, sa, and d mean anodic side of the SM/BGS boundary, cathodic side of the concentrated analyte zone, anodic side of the concentrated analyte zone, and detector, respectively.